Substrate Integrated Waveguide (SIW) Diplexer with Novel Input/Output Coupling and no Separate Junction

Augustine Onyenwe Nwajana[*], Amadu Dainkeh[1], Kenneth Siok Kiam Yeo[2]

[*,1,2]Department of Electrical and Electronic Engineering, University of East London, E16 2RD, London, UK

[*]a.nwajana@ieee.org, [1]u0925309@uel.ac.uk, [2]k.yeo@uel.ac.uk

Abstract—A microwave diplexer implemented by using the twenty-first century substrate integrated waveguide (SIW) transmission line technology is presented. No separate junction (be it resonant or non-resonant) was used in achieving the diplexer, as the use of an external junction for energy distribution in a diplexer normally increases design complexity and lead to a bulky device. The design also featured a novel input/output coupling technique at the transmit and the receive sides of the diplexer. The proposed SIW diplexer has been simulated using the full-wave finite element method (FEM), Keysight electromagnetic professional (EMPro) 3D simulator. The design has also been validated experimentally and results presented. Simulated and measured results show good agreement. The measured minimum insertion loss achieved on the transmit and the receive channels of the diplexer are 2.86 dB and 2.91 dB, respectively. The measured band isolation between the two channels is better than 50 dB.

1. INTRODUCTION

A diplexer is the simplest form of multiplexer that is widely used for either splitting a frequency band into two sub-bands of frequencies, or for combining two sub-bands into one wide frequency band [1]. As a frequency selective device, a diplexer connects two different networks with different operating frequencies to a single port. The increasing demand and high interest in size miniaturization, as well as reduction in design complexity of microwave components, have motivated a lot of researchers into seeking solutions and remedies to the ever growing challenges. Microwave diplexer is one of the essential components in the radio frequency (RF) front end of most multi-service and multi-band communication systems and sub-systems. This is because the presence of the diplexer reduces the number of antennas required in a system [2]. The RF front end of any cellular base station is a very good example of a system that has highly benefitted from the merits of achieving a diplexer with simple design and reduced size. The diplexer present in the RF front end of a cellular base station makes it possible for an input signal with two different frequencies, to split into two different signals at the output ports. It also facilitates the combination of two different input signals into one signal at the output port [3].

A wide range of planar and non-planar transmission line (TL) technologies have been utilised in the implementation of microwave diplexers. Some of the popular technologies that have been well researched and reported for diplexer implementation include slotline [4], stripline [5], coplanar waveguide [6], microstrip [7], waveguide [8, 9], and the substrate integrated waveguide [10]. Though diplexers

implemented with non-planar (e.g. waveguides) transmission lines have high Q-factor, low loss, and better power handling ability, they become bulky at lower frequencies [11]. Diplexers implemented with planar (e.g. slotline, stripline, coplanar waveguide, and microstrip) transmission lines, on the other hand, are more compact in size but suffer from low power handling abilities. SIW diplexers combine the advantages of both planar and non-planar transmission lines by being of small size, low cost, low loss and high Q-factor [12].

Substrate integrated waveguide [13] is a twenty-first century TL that has evolved to bridge the gap between planar and waveguide transmission lines. This new type of TL has changed the paradigm relating to the development of circuits, components, devices, sub-systems and systems operating in the microwave and millimetre-wave frequency range. The SIW is actually a planar structure with waveguide performance. This means that the SIW combines the merits of microstrip, i.e. compact size, low cost, easy to manufacture and easy integration with active devices; with the merits of waveguides, i.e. low radiation loss, high unloaded quality factor, and high power handling capabilities. [14] described the SIW as a dielectric-filled waveguide that is synthesized by two rows of metalized vias, embedded in a dielectric substrate with conductor claddings on the top and the bottom walls. Some other main merits of the substrate integrated waveguide, besides the high quality factor and high power handling capability include: its ability to integrate typical waveguide components in planar form, the flexibility of its design, and the comprehensive shielding of its structure. Substrate integrated waveguide devices can be manufactured or fabricated using different technologies such as: the printed circuit board, the low-temperature co-fired ceramics, the monolithic semiconductor, etc.

2. SIW CAVITY DESIGN

The substrate integrated waveguide cavity (i.e. resonator), according to [15], was first proposed by Piolote, Flanik and Zaki. They developed the idea of using a series of metallic posts (or via holes) through the substrate, to replace the waveguide walls. The idea did not change the effect of metallic walls, but gave rise to the SIW transmission line resonator / cavity. The SIW consists of two parallel rows of via holes embedded in the dielectric substrate as shown in Fig. 1 [16]; where w and l are the width the length of the SIW cavity, respectively, h is the thickness of the dielectric substrate, d is the diameter of the metallic post or via, and p is the pitch.

The fundamental frequency, f_{101} of the SIW cavity at its fundamental TE_{101} mode can be determined using (1) [17], where w_{eff} and l_{eff} are the equivalent width and length of the SIW cavity, respectively, μ_r is the relative permeability of the substrate, and c_0 is the speed of light in free space. The empirical formulae for calculating w_{eff} and l_{eff} are given in (2) and (3), respectively [18].

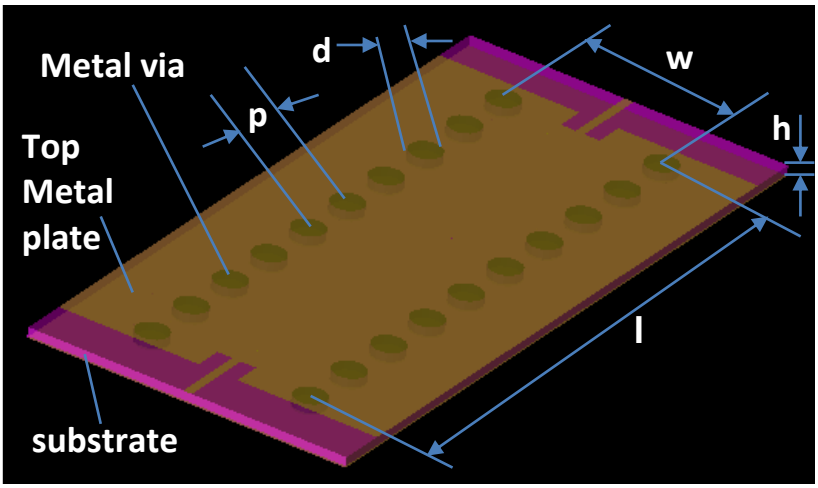

Figure 1. Structure of the SIW cavity / resonator [16].

$$f_{101} = \frac{c_0}{2\pi\sqrt{\mu_r \varepsilon_r}} \sqrt{\left(\frac{\pi}{w_{eff}}\right)^2 + \left(\frac{\pi}{l_{eff}}\right)^2} \tag{1}$$

$$w_{eff} = w - \frac{d^2}{0.95p} \tag{2}$$

$$l_{eff} = l - \frac{d^2}{0.95p} \tag{3}$$

3. DIPLEXER DESIGN

The microwave diplexer presented in this paper is based on the circuit model proposed in [19]. While [19] implemented the proposed circuit model using the traditional microstrip technology, the work presented in this paper employs the twenty-first century SIW transmission line technology for the diplexer implementation. The coupling arrangement for the proposed 10-pole diplexer, as reported in [19] is shown in Fig. 2, where D1 and D1' are the dual-band resonators designed using the technique reported in [20]. T2, T3, T4, T5 and R2, R3, R4, R5 are the sets of transmit (*Tx*) and receive (*Rx*) resonators for the first and the second passbands of the diplexer, respectively. The Tx and the Rx resonators were designed using the technique reported in [21].

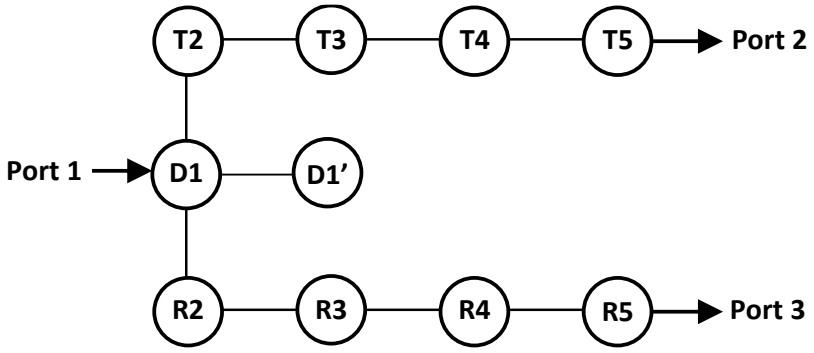

Figure 2. Coupling arrangement for the proposed 10-pole diplexer [18].

The D1 and D1' present in Fig. 2 can be viewed as the energy distributor (*ED*) which distributes energy towards the *Tx* and the *Rx* bands of the diplexer. This is because they replace the separate/external junctions (both resonant and non-resonant) used in most diplexer designs reported in literature. The actual function of the dual-band resonators is to establish the two passbands of the diplexer. D1 and D1' also contribute to the number of poles contained in the diplexer as explained in [19]. This is an advantage as it means that the proposed diplexer is relatively more compact when compared to conventional diplexers were resonant and non-resonant junctions are used for energy distribution.

3.1 DESIGN SPECIFICATIONS

The practical design parameters for the proposed diplexer are given in Tab. 1, where f is the centre frequency of the resonators/cavities used in the design. Rogers RT/Duroid 6010LM substrate, with relative permittivity ε_r = 10.8, substrate thickness h = 1.27 mm and relative permeability μ_r = 1 was employed in the design. A full-wave simulation layout and the responses, using Agilent electromagnetic professional (EMPro) finite-element method (FEM), for the *Tx*, *Rx* and *ED* cavities is shown in Fig. 3, where f_{Tx}, f_{Rx} and f_{ED} are the centre frequencies for the *Tx*, *Rx* and *ED* cavities, respectively.

Table 1. Practical design parameters for the substrate integrated waveguide diplexer component cavities

Cavity	f [GHz]	d [mm]	p [mm]	w [mm]	l [mm]
Tx	1.788	2.0	3.725	37.25	37.25
Rx	1.917	2.0	3.490	34.90	34.90
ED	1.849	2.0	3.609	36.09	36.09

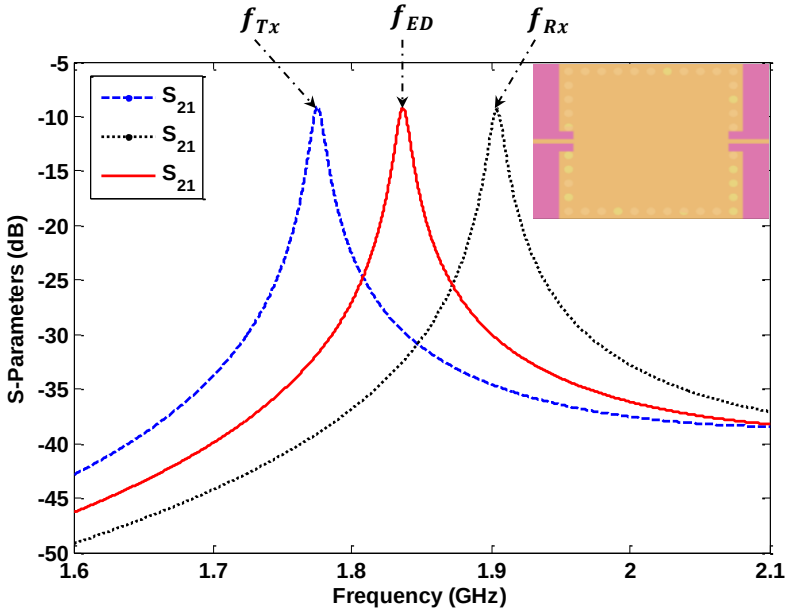

Figure 3. Layout and simulation responses for the *Tx*, *Rx* and *ED* cavities at their respective centre frequencies.

3.2 COUPLING COEFFICIENT EXTRACTION

The coupling between adjacent SIW cavities was achieved by simulating two cavities using the methods shown in Fig. 4. The full-wave simulation was conducted using the Agilent EMPro FEM 3D simulator. It is clear from Fig. 4 that an increase in the aperture size *s*, results to an increase in the coupling strength between the two cavities. Similarly, a reduction in the size, *s*, would lead to a reduction in the coupling strength between the two cavities.

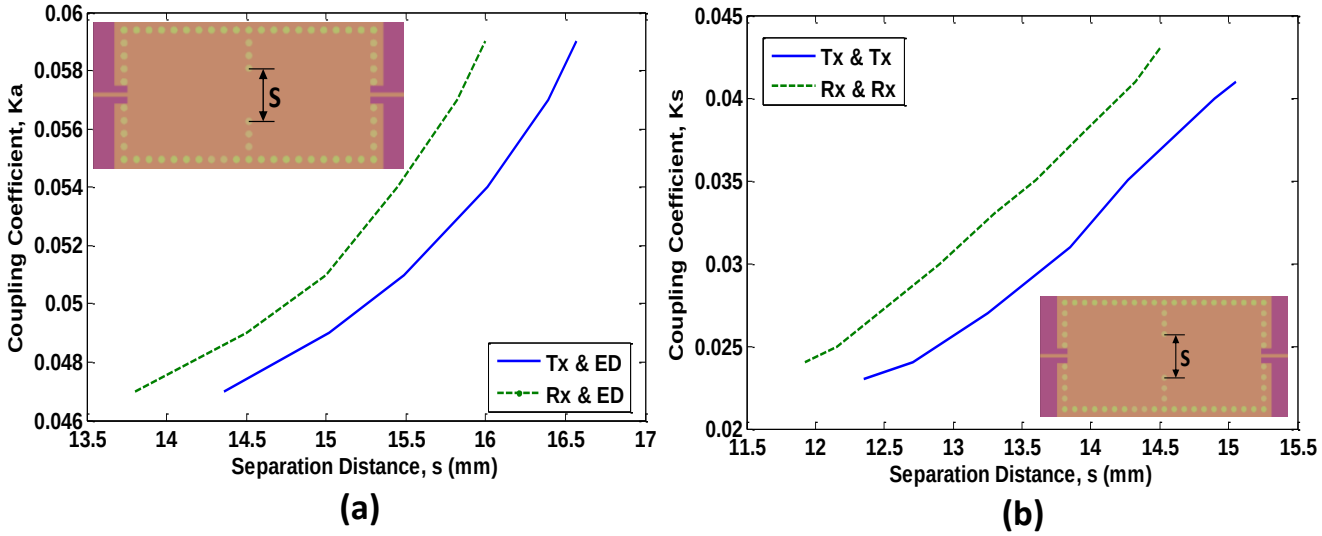

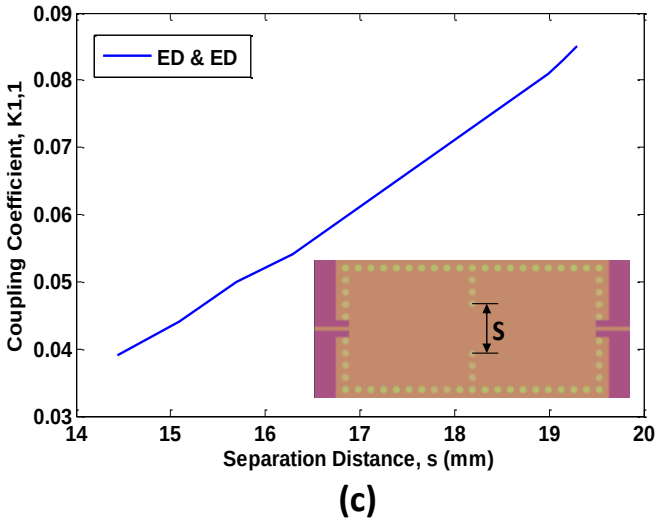

Figure 4. Coupling coefficient extraction technique for the SIW cavities. (a) *Tx* & *ED* and *Rx* & *ED* couplings. (b) *Tx* & *Tx* and *Rx* & *Rx* couplings. (c) *ED* & *ED* coupling.

The type of coupling shown in Fig. 4 (a) is known as asynchronous coupling since the two cavities involved are of different dimensions. This type of coupling is calculated using (4) derived from [22]. On the other hand, Fig. 4 (b) and Fig. 4 (c) show a coupling technique referred to as synchronous coupling. This is because the adjacent pair of cavities involved are exactly of the same dimension. This type of coupling (i.e. synchronous coupling) is calculated using (5) which is also derived from [22]. The parameters f_1 and f_2 in (4) and (5) are the eigen-modes from simulating coupled SIW cavities. The f_{r1} and f_{r2} parameters in (4) are the fundamental resonant frequencies of cavities 1 and 2, respectively. k_s and k_a are the synchronous and asynchronous couplings, respectively.

$$k_a = \frac{1}{2}\left(\frac{f_{r2}}{f_{r1}} + \frac{f_{r1}}{f_{r2}}\right)\sqrt{\left(\frac{f_2^2 - f_1^2}{f_2^2 + f_1^2}\right)^2 - \left(\frac{f_{r2}^2 - f_{r1}^2}{f_{r2}^2 + f_{r1}^2}\right)^2} \tag{4}$$

$$k_s = \frac{f_2^2 - f_1^2}{f_2^2 + f_1^2} \tag{5}$$

3.3 EXTERNAL QUALITY FACTOR EXTRACTION

The external quality factor, Q_{ext}, values for the *Tx*, the *Rx* and the *ED* components of the diplexer were determined as 24.285, 24.285, and 12.143, respectively. Two different techniques were employed in achieving the Q_{ext} values. The first technique, used in achieving the *Tx* and the *Rx* Q_{ext} values was first reported in [21]. This novel technique exploits the step impedance between the 50 Ohms input/output feedline and the transition to control the input/output couplings of the diplexer. Though the new transition

technique was first proposed in [21], it was only used in a simple 3-pole bandpass filter circuit in order to test its validity. In this paper, the proposed transition method has now been extended to a complex 10-pole diplexer circuit that operates at three different centre frequencies. The second technique, used in achieving the *ED* Q_{ext} value was proposed in [23]. This technique involves a transition from a coplanar waveguide (CPW) to the SIW, using a 90^o bend as shown in Fig. 5.

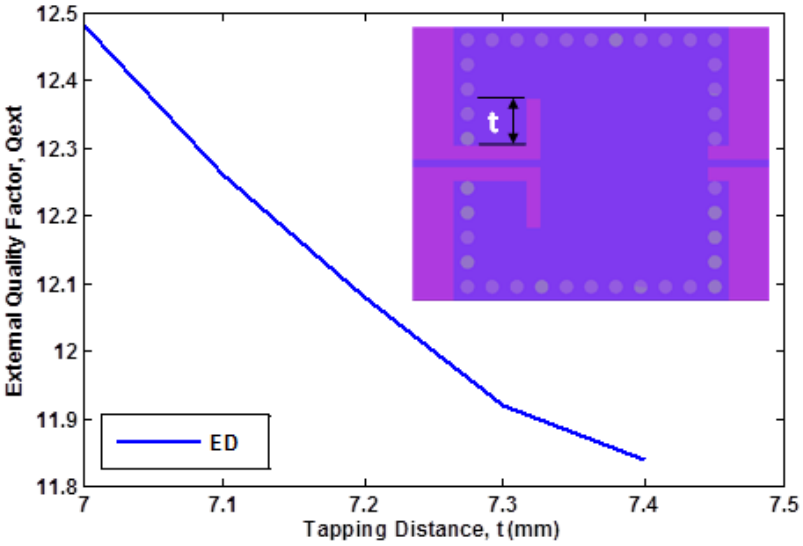

Figure 5. External quality factor extraction technique for the *ED* component of the SIW diplexer.

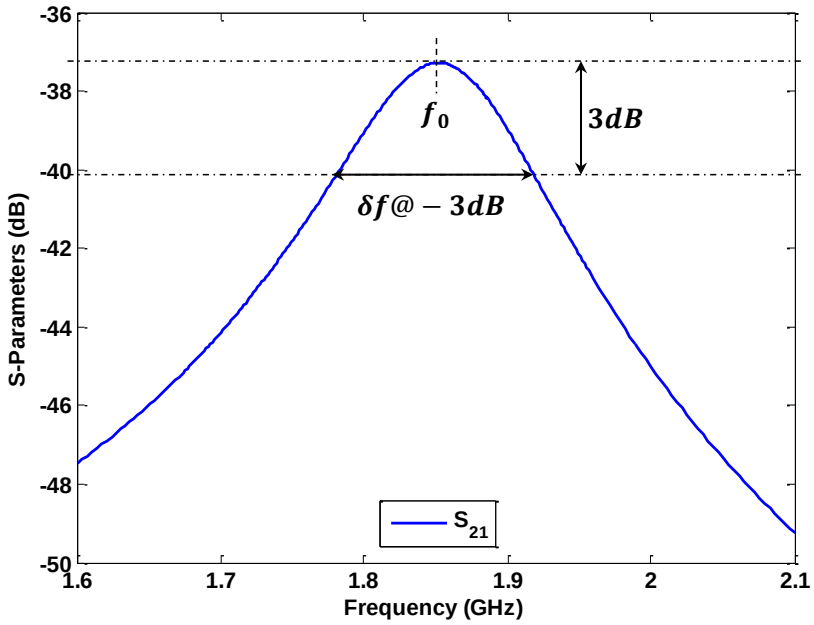

Figure 6. Simulation response of the transition from CPW to SIW using 90^o bend.

The simulated Q_{ext} value of the *ED* component can be determined from Fig. 6 which is based on (6); where f_0 is the fundamental resonant frequency of the cavity being simulated, and δf *@-3dB* is the 3 dB bandwidth of the simulated curve [24]. The simulated Q_{ext} values were achieved by adjusting the tapping distance, t as shown in Fig. 5. It can be seen from Fig. 5 that when t = 7.2 mm, Q_{ext} = 12.143. Hence, t = 7.2 mm is the required tapping distance value for the diplexer input/output, at the *ED* component.

$$Q_{ext} = \frac{f_0}{\delta f_{-3dB}} \tag{6}$$

4. SIMULATION

The layout of the 10-pole SIW diplexer, on a RT/Duroid 6010LM substrate is shown in Fig. 7. The substrate has a dielectric constant of 10.8, a relative permeability of 1.0 and a thickness of 1.27 mm. The physical dimensions of the diplexer are indicated in Fig. 7, with the corresponding design values for achieving the design presented in Tab. 2.

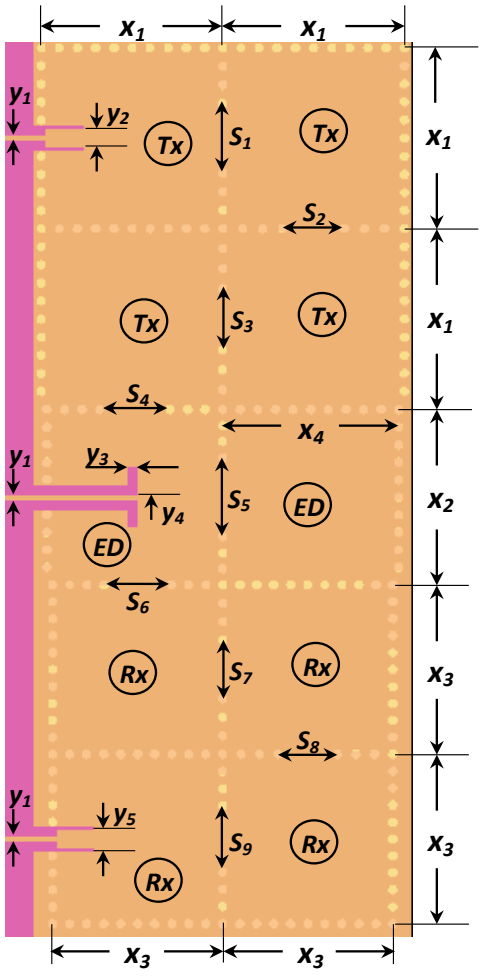

Figure 7. 10-pole SIW diplexer layout indicating physical dimensions, on a 1.27 mm thick RT/Duroid 6010LM substrate with a dielectric constant of 10.8.

Table 2. Physical dimensions of the proposed 10-pole substrate integrated waveguide diplexer.

Dimension	Value [mm]	Dimension	Value [mm]
x_1	37.25	s_1	14.27
x_2	34.90	s_2	12.71
x_3	36.09	s_3	12.71
x_4	34.90	s_4	15.02
y_1	1.12	s_5	16.29
y_2	3.70	s_6	14.50
y_3	2.00	s_7	12.16
y_4	9.20	s_8	12.16
y_5	3.70	s_9	13.60

In Fig. 7, the four cavities marked as *Tx* are resonating at the centre frequency of the diplexer transmit channel filter component (i.e. 1.788 GHz). The four other cavities marked as *Rx*, on the other hand, are resonating at the centre frequency of the diplexer receive channel filter component (i.e. 1.917 GHz). The remaining two cavities marked as *ED* are resonating at the centre frequency of the diplexer (i.e. 1.849 GHz). The function of the four *Tx* cavities is to establish the diplexer transmit band, while the four *Rx* cavities establish the diplexer receive band. The two *ED* cavities are responsible for energy distribution between the *Tx* and the Rx bands. The full-wave FEM simulation was performed using the Agilent (or Keysight) EMPro 3D simulator. All the loss parameters of the materials used in the design were included in the simulation.

One major issue observed while performing the simulation is the enormous amount of time it took the simulation to complete and return converged results. In order to significantly reduce the simulation time and achieve faster results convergence, all the circular metallic posts were replaced with 10-sided polygons (or decagons). This action reduced the simulation time by over 300%. The simulation time can also be greatly reduced by increasing the diameter of the metallic posts, as this would mean less number of metallic posts present in the design.

5. FABRICATION

The proposed 10-pole SIW diplexer was fabricated using the same material utilised in the finite-element method simulation. The fabrication was based on the PCB micro-milling process by means of the LKPF Protomat C60. Three Sub-Miniature-A (SMA) connectors were fixed onto the input and output ports of the fabricated diplexer as shown in Fig. 8. The SMA connectors serve as the points of connection between the diplexer and the Agilent Vector Network Analyzer during measurement. Notice that the three

ports of the SIW diplexer have been placed on the same side of the substrate. This is an added advantage as having the 3 ports on the side of the substrate would contribute to the diplexer physical size reduction.

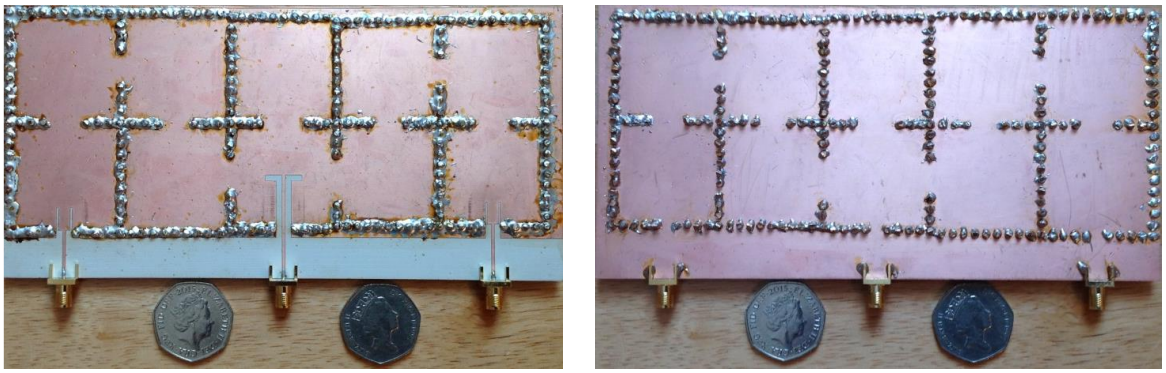

Figure 8. Photograph of the fabricated 10-pole SIW diplexer. (a) Top view. (b) Bottom view.

6. RESULTS

Both the simulation and the measurement results are mutually presented in Fig. 9 for easiness of comparison. It is clear from Fig. 9 that there is good agreement between the simulated and the measured results as both show minimum insertion losses across the diplexer transmit (i.e. S_{21}) and the diplexer receive (i.e. S_{31}) bands are 2.86 dB and 2.91 dB, respectively. The simulated band isolation (i.e. S_{32}) between the *Tx* and the *Rx* bands is at 46 dB, while the measured band isolation is about 50 dB. The simulated and measured return losses (i.e. S_{11}) are presented in Figure 10.

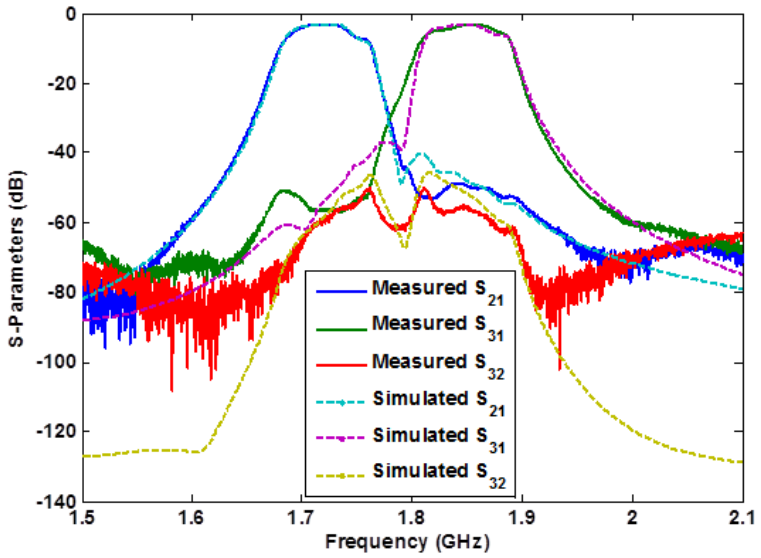

Figure 9. Comparison of the full-wave electromagnetic loss simulation responses and the measurement responses of the 10-pole SIW diplexer.

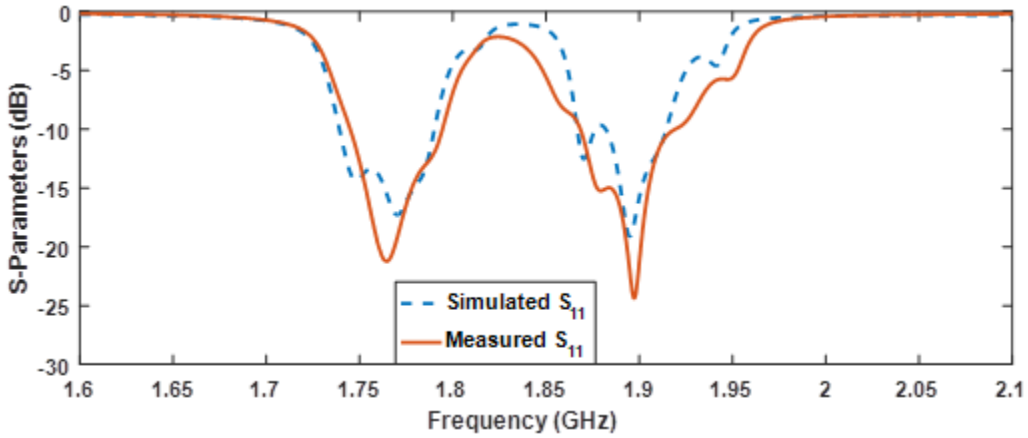

Figure 10. Simulated and measured insertion losses of the 10-pole SIW diplexer.

7. CONCLUSION

A SIW microwave diplexer has been achieved without using any separate junction for energy distribution. The design benefitted from two different types of SIW transition. The novel Microstrip-CPW-SIW transition proposed in [21] was utilised at the transmit and the receive ends of the diplexer, while a CPW-to-SIW transition with 90^{o} bend proposed in [23] was utilised at the energy distribution end of the diplexer. The design has been experimentally validated with the simulation and measurement results showing excellent agreement. The minimum insertion losses achieved on the SIW diplexer are 2.86 dB and 2.91 dB across the transmit and the receive bands, respectively. The unloaded quality factors for both passbands of the SIW diplexer, were determined to be 273 and 289 for the *Tx* and *Rx* bands, respectively. The minimum return loss recorded on the SIW diplexer results shown in Fig. 9 can be further improved by using more sided polygons for the metallic posts employed in the design. The down side is that the more the number of sides of the polygon used for the metallic post, the more time it would take for simulation results to converge, as more meshing would be performed during the FEM simulation.

REFERENCES

1. Zhu, L., R. R. Mansour, and M. A. Yu, "A compact waveguide diplexer employing dual-band resonators," *IEEE MTT-S International Microwave Symposium Digest*, 1−6, Tampa, FL, USA, June 2014.
2. Deng, H. W., Y. J. Zhao, F. Fu, X. J. Zhou, and Y. Y. Liu, "Compact and high isolation microstrip diplexer for GPS and UWB application," *IET Electronics Letters*, Vol. 49, No. 10, 659−661, May 2013.

3. Xiao, J.-K., M. Zhu, Y. Li, L. Tian, and J.-G. Ma, "High selective microstrip bandpass filter and diplexer with mixed electromagnetic coupling," *IEEE Microwave and Wireless Components Letters*, Vol. 25, No. 12, 781−783, December 2015.
4. Liu, H., W. Xu, Z. Zhang, and X. Guan, "Compact diplexer using slotline stepped impedance resonator," *IEEE Microwave and Wireless Components Letters*, Vol. 23, No. 2, 75−77, February 2013.
5. Xu, W.-Q., M.-H. Ho, and C. G. Hsu, "UMTS diplexer design using dual-mode stripline ring resonators," *IET Electronics Letters*, Vol. 43, No. 13, 721-722, June 2007.
6. Lai, C.-H., G.-T. Zhou, and T.-G. Ma, "On-chip miniaturized diplexer using jointed dual-mode right-/left-handed synthesized coplanar waveguides on GIPD process," *IEEE Microwave and Wireless Components Letters,* Vol. 24, No. 4, 245−247, April 2014.
7. Nwajana, A. O. and K. S. K. Yeo, "Multi-coupled resonator microwave diplexer with high isolation," In *Proceedings of the 46th European Microwave Conference (EuMC 2016),* 1167−1170, London, UK, October 2016.
8. Palma, L. D., F. Bilotti, A. Toscano, and L. Vegni, "Design of a waveguide diplexer based on connected bi-omega particles," *IEEE Microwave and Wireless Components Letters*, Vol. 22, No. 3, 126−128, March 2012.
9. Skaik, T. F., M. J. Lancaster, and F. Huang, "Synthesis of multiple output coupled resonator circuits using coupling matrix optimization," *IET Journal of Microwaves, Antenna & Propagation*, Vol. 5, No. 9, 1081−1088, June 2011.
10. Schorer, J., J. Bomemann, and U. Rosenberg, "Mode-matching design of substrate mounted waveguide (SMW) components," *IEEE Transactions on Microwave Theory and Techniques,* Vol. 64, No. 8, 2401−2408, August 2016.
11. Packiaraj, D., M. Ramesh, and A. T. Kalghatgi, "Cavity diplexer using tapped line interdigital filters. In *Proceedings of the 2005 Asia-Pacific Microwave Conference (APMC 2005),* 1−3, Suzhou, China, December 2005.
12. Adabi, A. and M. Tayarani, "Substrate integration of dual inductive post waveguide filter," *Progress in Electromagnetic Research B,* Vol. 7, 321−329, 2008.
13. Chen, X.-P. and K. Wu, "Substrate integrated waveguide filter: basic design rules and fundamental structure features," *IEEE Microwave Magazine,* Vol. 15, No. 5, 108−116, July, 2014.
14. Cheng, Y. J., *Substrate integrated antennas and arrays,* CRC Press, New York, 2015.
15. Han, S.-H., X. L. Wang, Y. Fan, Z. Q. Yang, and Z. N. He, "The generalized Chebyshev substrate integrated waveguide diplexer," *Progress in Electromagnetic Research,* Vol. 73, 29−38, 2007.
16. Nwajana, A. O., K. S. K. Yeo, and A. Dainkeh, "Low cost SIW Chebyshev bandpass filter with new input/output connection," In *Proceedings of the 16th Mediterranean Microwave Symposium (MMS 2016),* 1−4, Abu Dhabi, UAE, November 2016.
17. Chen, X., W. Hong, T. Cui, J. Chen, and K. Wu, "Substrate integrated waveguide (SIW) linear phase filter," *IEEE Microwave and Wireless Component Letters,* Vol. 15, No. 11, 787−789, November 2005.
18. Deslandes, D. and K. Wu, "Accurate modelling, wave mechanisms, and design considerations of a substrate integrated waveguide," *IEEE Transactions on Microwave Theory and Techniques,* Vol. 54, No. 6, 2516−2526, June 2006.
19. Nwajana, A. O. and K. S. K. Yeo, "Microwave diplexer purely based on direct synchronous and asynchronous coupling," *Radioengineering,* Vol. 25, No. 2, 247−252, June 2016.
20. Yeo, K. S. K. and A. O. Nwajana, "A novel microstrip dual-band bandpass filter using dual-mode square patch resonators," *Progress in Electromagnetic Research C*, Vol. 36, 233-247, January 2013.

21. Nwajana, A. O., A. Dainkeh, and K. S. K. Yeo, "Substrate integrated waveguide (SIW) bandpass filter with novel microstrip-CPW-SIW input coupling," *Journal of Microwaves, Optoelectronics and Electromagnetic Applications,* Vol. 16, No. 2, 393−402, June, 2017.
22. Hong, J.-S., *Microstrip Filters for RF/microwave applications* 2nd ed., Wiley, New York, 2011.
23. Deslandes, D. and K. Wu, "Integrated transition of coplanar to rectangular waveguides," *IEEE MTT-S International Microwave Symposium Digest,* 619−622, Phoenix, AZ, USA, May 2001.
24. Dainkeh, A., A. O. Nwajana, and K. S. K. Yeo, "Filtered power splitter using microstrip square open loop resonators," *Progress in Electromagnetic Research C,* Vol. 64, 133−140, May 2016.